Clin Neuroradiol (2021) 31:953–967
https://doi.org/10.1007/s00062-021-01057-7

REVIEW ARTICLE

Systematic Review of Different Neuroimaging Correlates in Mild Cognitive Impairment and Alzheimer's Disease

Puneet Talwar[1] · Suman Kushwaha[1] · Monali Chaturvedi[2] · Vidur Mahajan[3]

Received: 19 November 2020 / Accepted: 18 June 2021 / Published online: 23 July 2021

Abstract

Alzheimer's disease (AD) is a heterogeneous progressive neurocognitive disorder. Although different neuroimaging modalities have been used for the identification of early diagnostic and prognostic factors of AD, there is no consolidated view of the findings from the literature. Here, we aim to provide a comprehensive account of different neural correlates of cognitive dysfunction via magnetic resonance imaging (MRI), diffusion tensor imaging (DTI), functional MRI (fMRI) (resting-state and task-related), positron emission tomography (PET) and magnetic resonance spectroscopy (MRS) modalities across the cognitive groups i.e., normal cognition, mild cognitive impairment (MCI), and AD. A total of 46 meta-analyses met the inclusion criteria, including relevance to MCI, and/or AD along with neuroimaging modality used with quantitative and/or functional data. Volumetric MRI identified early anatomical changes involving transentorhinal cortex, Brodmann area 28, followed by the hippocampus, which differentiated early AD from healthy subjects. A consistent pattern of disruption in the bilateral precuneus along with the medial temporal lobe and limbic system was observed in fMRI, while DTI substantiated the observed atrophic alterations in the corpus callosum among MCI and AD cases. Default mode network hypoconnectivity in bilateral precuneus (PCu)/posterior cingulate cortices (PCC) and hypometabolism/hypoperfusion in inferior parietal lobules and left PCC/PCu was evident. Molecular imaging revealed variable metabolite concentrations in PCC. In conclusion, the use of different neuroimaging modalities together may lead to identification of an early diagnostic and/or prognostic biomarker for AD.

Keywords Magnetic resonance imaging · Functional MRI · Voxel-based morphometry · Diffusion tensor imaging · Positron emission tomography · Magnetic resonance spectroscopy

Introduction

Alzheimer's disease (AD) is a dynamic disorder. Sporadic or late-onset AD accounts for 60–70% of 50 million individuals with dementia globally with an incidence rate of around 10 million cases in the year 2018 alone [1, 2]. The pathophysiological mechanisms of AD occur much earlier than the clinical phenotypic manifestation. Identifying disease symptoms or predictors at its early stage is of significant interest in AD research.

In typical AD, the progression of clinical symptoms follows a sequential order, namely episodic memory loss, semantic memory loss, aphasic, apraxic, and visuospatial symptoms and finally, motor and visual deficits that correspond to the topographic progression of neuronal degeneration (hippocampus [HIP] and medial temporal lobe [MTL], posterior cingulate cortex [PCC] → lateral temporal cortex → frontal, temporal, and parietal neocortex → sensorimotor and occipital cortex) [3]. Since AD

The authors P. Talwar and S. Kushwaha contributed equally to the manuscript.

✉ Puneet Talwar
talwar.puneet@gmail.com

✉ Suman Kushwaha
sumankushwaha@gmail.com

[1] Department of Neurology, Institute of Human Behaviour and Allied Sciences (IHBAS), 110095 Dilshad Garden, Delhi, India

[2] Department of Neuroradiology, Institute of Human Behaviour and Allied Sciences (IHBAS), 110095 Dilshad Garden, Delhi, India

[3] Centre for Advanced Research in Imaging, Neuroscience and Genomics (CARING), Mahajan Imaging, New Delhi, India

Table 1 Approaches for identification of Neuroimaging biomarker for AD risk

Modality	Principle	Use	Clinical utility in AD
MRI (T1 weighted)	Technique that involves a magnetic field and radio waves to create detailed images of the tissues using signals from ^{1}H (proton) nuclei in water and fat over thousands of voxels	Structural visualization of gray matter, white matter and cerebrospinal fluid	Gray matter atrophy beginning in the medial temporal lobe and progressing to the temporal neocortex, parietal cortex and frontal cortex
rs-fMRI	Used to study the brain's functional organization based on the BOLD signal fluctuation	Measures spontaneous fluctuations in the blood oxygen level-dependent (BOLD) signal	Decreased functional hippocampal connectivity to the prefrontal cortex and cingulate cortex
DTI	MRI-based neuroimaging technique that relies on signals from water protons and enables in vivo quantification of differences in molecular diffusion at the cellular level	Used to visualize the location, orientation, and anisotropy of the brain's white matter tracts	Anatomical distribution of white matter microstructural damage in the early stages of AD
PET	Nuclear medicine functional imaging technique that uses radiation and radiotracer	Measure regional brain glucose metabolism; amyloid deposition in the brain	Regional brain glucose hypometabolism; Amyloid detection in AD brain
MRS	Uses spectra in a small number of voxels reflecting small metabolite molecules differentiated by their chemical shifts (δ)	Detects the chemical composition of the scanned tissue	Regional metabolite concentration in AD brain

MRI magnetic resonance imaging, *rs-fMRI* resting stage functional magnetic resonance imaging, *DTI* diffusion tensor imaging, *BOLD* blood oxygenation level dependent, *PET* positron emission tomography, *MRS* magnetic resonance spectroscopy, *AD* Alzheimer's disease

probably develops many years before clinical phenotypic symptoms manifest [4] and cognitive deficits are evident before the appearance of a full-blown dementia syndrome, mild cognitive impairment (MCI), a preclinical transitional state between normal cognition and AD phenotype, has drawn much attention in the recent past [5, 6].

Neuroimaging has evolved from an investigation for excluding the secondary causes of dementia to a modality required for establishing the diagnosis in the preclinical stage and tracking disease progression. Magnetic resonance imaging (MRI) techniques, mainly voxel-based morphometry (VBM), have provided an efficient and noninvasive way to quantify volumetric brain atrophy caused by gross neuronal loss. At the same time, the integrity of white matter (WM) fiber tracts within axonal projections can be assessed in vivo using diffusion tensor imaging (DTI) [7]. The use of VBM and region of interest (ROI) identifies structural MRI alterations while DTI is sensitive to WM microstructure change, such as degeneration of myelin and axons. The integrity of WM is best assessed with fractional anisotropy (FA), which mirrors fiber density, axonal diameter and myelination [8]. In vivo neuroimaging in humans provides a richer understanding of the pathophysiology of AD. A wide range of neuroimaging modalities are now available to perform multimodality analyses assessing interrelationships between different pathophysiological processes.

Several studies have demonstrated that baseline MRI scans can precisely detect patterns of cerebral atrophy in AD [3, 9–12]. Compared to conventional functional MRI (fMRI) studies, resting-state fMRI (rs-fMRI) is a task-free technique that can be easily used in cognitively impaired individuals. The disruptive structural connectivity, the interneuronal connections forming networks between brain regions, may exacerbate the effect of molecular pathology on cognitive functions in AD [13]. Previous DTI and rs-fMRI studies have identified consistent structurally and functionally connected brain networks in the human brain [14, 15].

The emerging positron emission tomography (PET) imaging strategies have integrated the advantages of PET and MR to diagnose and monitor AD. Fluorodeoxyglucose-positron emission tomography (FDG-PET) and amyloid PET (^{11}C-Pittsburgh compound B and ^{18}F-labelled amyloid tracers) are the most commonly available modalities for AD detection [16, 17]. The combination of PET with other imaging modalities can improve the diagnostic accuracy of dementia. Other than CT, MRI and PET, proton magnetic resonance spectroscopy (^{1}H-MRS) monitors metabolic changes associated with AD in the brain. It is a noninvasive and inexpensive neuroimaging modality that does not require use of radiotracers [18].

Although different neuroimaging modalities have been used to identify early diagnostic and prognostic factors, there is no consolidated view of the findings. It is believed that a single neuroimaging biomarker cannot predict early AD risk and the conversion of MCI subjects into AD due to the complex and multifactorial nature of AD. Different neuroimaging studies have identified the association of different brain regions with AD. Several meta-analysis studies covering various aspects of the cognitive spectrum in aging and diseases have been published. Here, we provide a comprehensive review of 46 quantitative meta-analysis studies involving different neuroimaging modalities evalu-

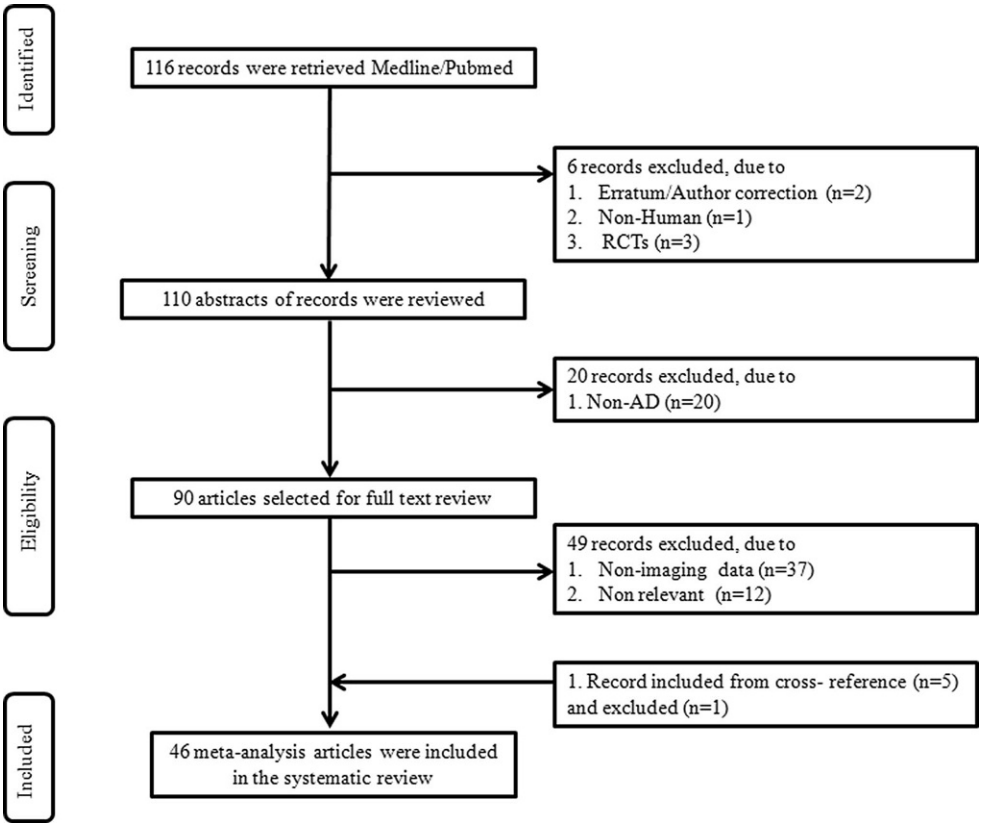

Fig. 1 Flow diagram representing the selection of studies for systematic review. *RCTs* randomized controlled trials, *AD* Alzheimer's disease

ating the neural correlates in AD and/or MCI. Different neuroimaging modalities for the identification of neuroimaging biomarkers for AD risk are shown in Table 1.

Methods

Medline/PubMed was searched to retrieve articles up to 31 December 2019 with the following search string: ("meta-analysis"[title]) AND ("Alzheimer's disease" OR "mild cognitive impairment" OR "MCI") AND ("imaging" OR "MRI" OR "structural MRI" OR "DTI" OR "Diffusion-weighted imaging" OR "Diffusion tensor imaging" OR "fMRI" OR "functional MRI" OR "MRS" OR "CT" OR "PET" OR "SPECT"). Cross-references of previously published review articles and included articles were hand searched to find any additional relevant studies. The articles written only in the English language were included in the study.

The meta-analysis studies were selected based on the following inclusion criteria: quantitative data from any neuroimaging modality namely MRI, DTI, fMRI, PET, MRS reporting coordinates in Montreal Neurological Institute (MNI) or Talairach space, studies having patients with AD and/or MCI and meta-analysis studies with total included studies more than four. Both observational and longitudinal studies with quantitative and/or functional data were considered. After excluding all non-English articles, titles/abstract screening was done by two authors independently (PT and MC). Articles not excluded by any investigator were studied in detail, and a final decision was taken after consensus with a third investigator (SK). The flow diagram representing the selection of studies for meta-analysis is provided in Fig. 1.

Results

Study Search, Characteristics and Findings

The literature search yielded 116 references, out of which 110 potentially relevant citations were reviewed after removing 2 erratum/author corrections, 1 non-human article, 3 randomized clinical trials (RCTs). After screening all the titles and abstracts, 90 articles were selected for full-text review. Out of the 90 articles 41 meta-analysis studies met the inclusion criteria, including relevance to mild cognitive impairment and/or AD along with neuroimaging modality used with quantitative data analysis. Of the records 5 were included from the cross-references making 46 articles eligible for final inclusion in our meta-analysis.

The study characteristics from all 46 studies are provided in Table S1. Among the 46 selected meta-analysis articles, 23 studies included patients with AD (PwAD), 15 had patients with MCI (PwMCI), 9 included data associated with progression to AD and included 8 studies with mixed phenotype.. The number of datasets with different neuroimaging modalities involving PwAD was MRI 13, DTI 2, fMRI 5, PET 3, MRS 1 and MRI 5, DTI 1, fMRI 8, PET 2, MRS 1 for PwMCI from included studies. The most common method used for quantification was the anatomical likelihood estimation (ALE). A detailed comparison of results from 46 meta-analysis studies with different neuroimaging methods under review is provided in Supplementary file 1.

Discussion

With the burgeoning advances of neuroimaging techniques in recent years, there is an exponential increase in research and literature on AD which emphasizes the need to identify, assess and amalgamate the findings from several meta-analysis studies to be maximally informed with minimal bias. The summary of the significant inferences from different neuroimaging modalities associated with MCI, AD, and MCI to AD progression is provided in Table 2.

Neural Correlates from MRI in MCI and AD

The whole-brain VBM is a computational approach that can measure group differences in the density or volume of the brain and local concentrations in brain tissue through a voxel-wise comparison of multiple MRI images [19]. Although several manual, semi-automatic, and fully automatic computational approaches are available for assessing volumetric brain measurements [20], knowledge of the pathophysiology is vital to evaluate the imaging features. Deposition of amyloid beta (Aβ) and neurofibrillary tangles (NFTs) set off a cascade of a neurodegenerative process reflected neuroanatomically as volume loss and atrophy. Neuropathological studies have staged the AD according to the occurrence of NFTs and neuropil threads into transentorhinal stages I–II (affecting transentorhinal cortex) followed by limbic stages III–IV (involving entorhinal region/hippocampal formation proper) and then isocortical stages V–VI, which subsequently affects all isocortical association areas. Transentorhinal and limbic stages were associated with MCI, while stage IV onwards is associated with AD implying spread beyond the MTL. Limbic structures that are relatively spared in normal aging are the key regions affected early in the course of AD [21].

Atrophy of the MTL has been the primary focus of volumetric analysis by MRI in AD [22]. We observed that the previous studies focused not only on identifying and analyzing grey matter (GM) and WM regional volume loss in MTL but also on identifying auxiliary areas affected beyond the MTL in MCI and AD and areas affected during disease progression. The summarized grey matter and white matter changes in MCI and AD are depicted in Fig. 2.

Several meta-analytical studies have confirmed cortical thinning and volume loss of bilateral MTL (HIP, parahippocampal gyrus [PHG], amygdale, uncus, entorhinal cortex [EC]), precuneus, and PCC as the imaging signatures for AD [23–25]. In addition to bilateral MTL, GM atrophy of MTL, thalamus, and cingulate cortex was observed in MCI while AD had an extensive GM deficit involving both cortical and subcortical regions (parietal, frontal and insular cortices and including bilateral caudate nuclei). Such affection of the neocortices suggests additional neural networks beyond memory networks on AD as compared to MCI [25, 26]. Although insular subregional atrophy was found to be non-specific to one neurodegenerative disease, left anterior insular cortex atrophy was greater in frontotemporal dementia (FTD) whereas larger clusters of atrophy were observed in the right anterior dorsal insular cortex in AD and Parkinson's disease (PD)/dementia with Lewy bodies (DLB). Furthermore, right dorsal atrophy was found to be associated with perception and cognitive deficits, and left anterior insular cortex atrophy with speech, emotion, and affective cognitive deficits [27]. It has been suggested that in AD, besides atrophy, additional imaging markers such as abnormally low parietal glucose utilization and perfusion should be considered for better diagnosis and subtype characterization mainly in dissociating AD and frontotemporal lobar degeneration (FTLD) [28].

Although reduction of the bilateral HIP volume is not specific to AD and is exhibited by other brain disorders, atrophy in the left anterior HIP and bilateral PCC is found to be specific to AD as superior frontal gyrus (SFG) and ventromedial frontal cortex is found to be atrophied in late life depression (LD). This explains the differential involvement of visual spatial implicit memory and topographical memory in AD and executive deficits in LD [23]. Similarly, global HIP atrophy is observed in AD with the posterior portion being more atrophic while in semantic dementia (SD), atrophy was limited to the anterior portion. This explanation supports the differential involvement of neural networks of anterior and posterior HIP and suggests that atrophy of posterior HIP and posterior medial brain regions are associated with episodic memory deficits observed in AD [29]. The significance of HIP atrophy in AD as a possible early neuroanatomical biomarker has been studied extensively by volumetric approaches [29] and HIP deterioration was seen in early AD while affection of MTL and anterior cingulate gyrus was observed in AD of longer duration/later stages of AD [24]. Wang et al. reported significant GM volume reductions in the limbic regions (left PHG

Table 2 Summary of major findings from different neuroimaging modalities associated with MCI, AD and MCI to AD progression

	MCI	AD	MCI to AD progression
MRI			
GM	Transentorhinal and HIP region [21]	Memory impairment is a more accurate predictor of early AD than atrophy of MTL [94]	Transentorhinal and HIP region [21]
	Atrophy in the bilateral MTL involving bilateral HIP and amygdala, the left PHG and the left uncus [26]	Left HIP atrophy [33]	Left MTL (including PHC, amygdala and HIP) [25]
	Right lateralized atrophy of HIP [33]	Early stage HIP deterioration, Late stage MTL and the anterior cingulate gyrus [24]	Left MTL atrophy especially anterior HIP and PHG of left hemisphere [40]
	Atrophy of genu and rostrum of corpus callosum (CC) [38]	Left anterior HIP and bilateral PCC [95]	*APOE* ε4 was associated with atrophic HIP volume [96]
	2.2-fold higher volume loss in the HIP, estimated mean HIP atrophy rates were 2.53%/year for MCI, 1.12%/year for controls, and 1.35%/year for MCI after removing the effect attributable to normal aging; only *APOE* ε4 (not age and gender) was a significant moderator of atrophy rate [32]	Posterior HIP and precuneus [29] Annualized HIP atrophy rate of 4.6% [31] HIP, amygdala, and entorhinal cortex volume reduction [34] Atrophy of splenium along with genu and rostrum of CC [38] Frontomedian-thalamic network involvement [21] Atrophy in Crus I/II and lobule VI of cerebellum [36] GMV atrophy in limbic regions (left PHG and left posterior cingulate gyrus) and decreases in right fusiform gyrus and right superior frontal gyrus [30] Within the AD coatrophy network, coaltered areas including the left HIP, bilateral amygdala, right PHG, and right temporal inferior gyrus were identified as pathoconnectivity hubs [23]	The entorhinal cortex atrophy measure on MRI is comparable in prediction value to amyloid PET [41]
WM	–	WM reductions in bilateral inferior temporal gyrus, splenium of CC, right PHG and HIP along with left caudate nucleus, left superior corona radiata, and right inferior temporal gyrus [8]	–
DTI	Reduced FA in fornix and UF with increased MD in genu and splenium of CC, UF and PHC along with significant FA decrease in the posterior corona radiate [46]	Increased MD of HIP was more sensitive indicator of poor verbal and memory performance than HIP volume [35]	WM integrity precede the atrophic changes [35]
		Decreased FA in left posterior limb of internal capsule, left anterior corona radiata, left thalamus, and left caudate nucleus along with left caudate nucleus, left superior corona radiata, and right inferior temporal gyrus [34]	Reduced FA fornix and UF with increased MD in genu and splenium of CC, UF and PHC [46]

and left posterior cingulate gyrus) in PwAD [30]. Barnes et al. studied the HIP volume atrophy rates and reported the annualized HIP atrophy rate of 4.6% in PwAD compared to 1.4% in HC [31]. Tabatabaei-Jafari et al. showed a 2.2-fold higher volume loss in the hippocampus in MCI participants than matched healthy people of the same age and was associated with risk factors including *APOE* ε4 genotype and female gender [32]. Interestingly, two other studies noted right lateralized atrophy of HIP in MCI against AD, which displayed left-sided biased HIP GM loss [25, 33].

It has also been demonstrated that the HIP GM atrophy is followed by WM atrophy in areas involved in the memory network, such as the HIP, amygdala, and EC [34]. The succession of WM atrophy likely occurs through demyelination as these areas have efferent connections mainly from HIP and amygdala [34]. Furthermore, the role of microvas-

Table 2 (Continued)

	MCI	AD	MCI to AD progression
fMRI			
rs-fMRI	Reduced resting-state activity in the PCC, right angular gyrus, right PHG and left fusiform gyrus. Hypoactivation in the PCC is independent of the GM volume alterations and specific to aMCI compared to svMCI [59]	MTL activity deficits across encoding and retrieval paradigms and greater activity in DL-PFC and VL-PFC during encoding and retrieval tasks (possibly compensatory) [60]	–
	Decreased ALFFs in the bilateral precuneus/PCC, bilateral frontoinsular cortices, left occipitotemporal cortex, and right supramarginal gyrus and increased ALFFs in the right lingual gyrus, left middle occipital gyrus, left HIP, and left inferior temporal gyrus [53]	DMN hypoconnectivity in the DMN (precuneus [PCu] and posterior cingulate cortex [PCC]), salience network hyperconnectivity (anterior insula), and hypoconnectivity in the visual cortex [58]	
	Decreased resting-state activity than HC in the left STG, right posterior cingulate/precuneus, uncus and hyperactivation in the inferior parietal lobule, superior parietal lobule [26]		
	DMN hyperconnectivity in the DMN (PCu and PCC) and LIM (HIP and EC) [58]		
	DMN hypoconnectivity in bilateral precuneus/PCC and MTL than HC [57]		
Task-based-fMRI	Decreased activation was mainly detected in frontoparietal and default mode networks [55]	Hypoactivation voxels in visual network [55]	–
	Increased activation in right HIP (mainly CA 2–4 subregions) during encoding tasks, decreased activation in the left HIP (at first predominantly cornu Ammonis (CA1), later also SUB and PHG) and fusiform gyrus during retrieval tasks, as well as attenuated activation in the right anterior insula/inferior frontal gyrus during verbal retrieval [61]	Hyperactivation within the precuneus during encoding tasks was accompanied by attenuated right hippocampal activation during retrieval tasks. Decreased MTL activation in severe AD is accompanied by stronger activation during memory encoding tasks in the precuneus [61]	
	Hypoactivation in the left inferior parietal lobule, right posterior cingulate, the bilateral precuneus and hyperactivation in the left middle frontal gyrus, superior parietal lobule, insula, STG and right inferior frontal gyrus [26]	Bilateral angular and the MTL, or superior frontal gyri demonstrated as the primary target for DMN modulation by brain stimulation [63]	
PET			
FDG-PET	Hypometabolism/hypoperfusion in inferior parietal lobules and precuneus [21]	Abnormally low parietal glucose utilization [28]	Better than structural MRI and SPECT [21]
			Hypometabolism/hypoperfusion in inferior parietal lobules and precuneus [21]
Amyloid-PET	–	Amyloid positivity decreases with age in PwAD (greatest in *APOE*4 non-carriers) and increase with age in other dementia subtypes [72]	Positive PiB increases risks by 3.7 times with mean follow-up duration ranging from 1–3.8 years [74]
			APOE ε4 was associated with increased cerebral amyloid deposition and cerebral hypometabolism [96]
			Hypometabolism in the left PCC/precuneus [67]

Table 2 (Continued)

	MCI	AD	MCI to AD progression
TSPO	Increased TSPO levels, mainly within the neocortex [75]	Increased TSPO levels throughout the brain especially within frontotemporal regions compared to controls [75]	–
MRS	Raised myoinositol (mI) concentration and choline/creatine ratio (Cho/Cr) along with reduced NAA level and NAA/mI ratio in the PC. Reduced NAA, creatine and choline with raised mI/Cr ratio in HIP with reduction in NAA and creatine in PWM [77]	Reduced NAA in PCC, bilateral hippocampus and decreased NAA/Cr (creatine) ratio markedly in the PC with elevated myoinositol (mI)/Cr ratio in PC and parietal gray matter [81]	–

MCI mild cognitive impairment, *aMCI* amnestic MCI, *AD* Alzheimer's disease, *PwAD* patients with AD, *GM* grey matter, *WM* white matter, *MTL* medial temporal lobe, *HIP* hippocampus, *PCC* posterior cingulate cortices, *PHC* parahippocampal cingulum, *PHG* parahippocampal gyrus, *FA* fractional anisotropy, *MD* mean diffusivity, *UF* uncinate fasciculus, *svMCI* subcortical vascular MCI, *ALFFs* amplitude of low-frequency fluctuations, *DL-PFC* dorsolateral prefrontal cortex, *VL-PFC* ventrolateral prefrontal cortex, *FDG-PET* fluorodeoxyglucose-positron emission tomography, *PiB* 11C-Pittsburgh Compound B, *DMN* default mode network, *MRI* Magnetic resonance imaging, *SPECT* single-photon emission computed tomography, *NAA* N-acetyl aspartate, *PWM* paratrigonal white matter, *LIM* limbic networks, *TSPO* translocator protein, *APOE* apolipoprotein E, *SUB* subiculum, *PCu* precuneus, *STG* superior temporal gyrus, *CC* corpus callosum

cular alteration and neuro-inflammatory processes, damage to myelin, abnormal lipid metabolism, and genetic influences have also been implicated in the WM damage [34].

Although memory impairment alone has been shown to predict early AD more accurately than atrophy of MTL on MRI, MTL atrophy in volumetric studies differentiated AD from HC and MCI from HC. For AD, an effect size of medial temporal lobe atrophy (MTA) score, HIP, EC, and PHG was large and significant than DTI [35]. In AD, consistent unique patterns of GM atrophy that were highly specific to underlying neuropathology were observed in the cerebellum. Atrophy was reported in crus I/II and lobule 6 of the cerebellum that shares connections with HIP and prefrontal regions and also participates in the executive control network (ECN), default mode network (DMN) and salience network (SN); however, this could be attributed to atrophic areas of the cerebral cortex which later affect the cerebellum as the association of cognitive impairment with cerebellar atrophy are inconsistent [36].

In AD, GM alterations follow a specific distribution pattern called coatrophy network based on the functional overlap at the molecular level among different brain regions. The core subnetwork in AD includes left HIP, left and right amygdala, right PHG, and right inferior temporal gyrus [23]. Additionally, VBM studies have identified consistent WM damage in cortico-cortical and cortico-subcortical connections contributing to cognitive impairment in AD patients [34]. In an interesting study, Wang et al. suggested that the extent of cognitive deficits in MCI and AD was directly related to the atrophy of the corpus callosum (CC). Being a major commissural pathway and the most extensive WM fiber bundle, it plays vital role in integrating perception and action. The splenium mediates loco-global facilitation from redundant targets [37]. Atrophy of genu and rostrum of CC was observed in PwMCI, while PwAD had additional atrophy of splenium. Furthermore, the degree of atrophy corresponded to the severity in mild and moderate AD [38]. It appears that in severe AD, the atrophy of the CC might reflect the cortical atrophy, which can be explained based on the Wallerian degeneration hypothesis [39].

Several studies identified potential markers for predicting conversion from MCI to AD and thereby, disease progression. One study concluded that left MTL atrophy especially anterior HIP and PHG of the left hemisphere, was an important and consistent neuroanatomical marker [40] while other suggested that EC is a more sensitive volumetric discriminator [35]. Seo et al. revealed that the MRI-based volumetric EC atrophy is comparable to amyloid PET in predicting conversion to AD [41]. Wang et al. on the other hand, emphasized the importance of mid-sagittal area changes in CC to indicate disease progression [38].

Neural Correlates from DTI in MCI and AD

In neuroimaging, DTI has been used to examine the subvoxel, microstructural properties and organization of WM by assessing the movement of randomly diffusing water molecules. In particular, measures of fractional anisotropy (FA) can be used to estimate the anisotropy (i.e. degree of directional coherence) of the underlying tissue structures in any given voxel, reflecting the strength of neuronal projections, while mean diffusivity (MD) or apparent diffusion coefficient (ADC) can be used to estimate relative tissue compactness and degree of myelination. Other DTI measures include the axial (diffusion rate along the main axis), and radial (rate of diffusion in the transverse direction) diffusivity. Diffusion in WM is less restricted along the axon and tends to be anisotropic, whereas in GM it is usually less anisotropic and, in the cerebrospinal fluid biomarker (CSF), is unrestricted in all directions (isotropic). Axonal

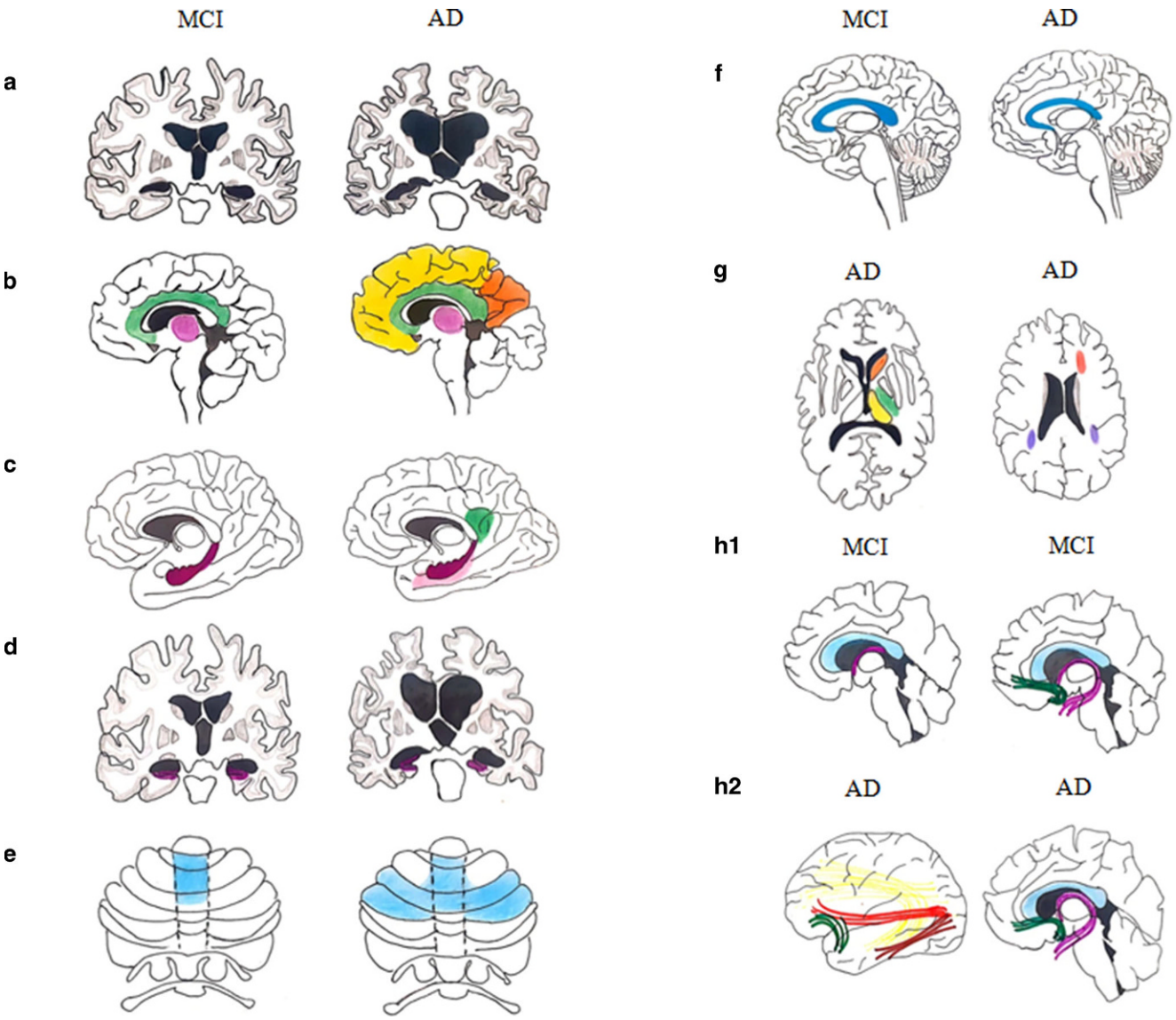

Fig. 2 Schematic representation of inferences from the various meta-analytical studies. Grey matter and white matter changes in MCI and AD. A Coronal section through the hippocampus at the level of the anterior pons showing medial temporal atrophy in MCI and AD. b Mid sagittal section showing grey matter atrophy of thalamus (*pink*) and cingulate cortex (*green*) in MCI besides MTL and grey matter atrophy in AD involving parietal (*orange*), frontal (*yellow*) and insular cortices besides thalamus, cingulate cortex and MTL. c Medial aspect of cerebral hemisphere in sagittal section showing grey matter volume loss in limbic regions involving hippocampus (*purple*) in MCI/early AD and affecting hippocampus (*purple*), parahippocampus (*pink*) and posterior cingulate cortex (*green*) in AD. d Coronal section in a plane through the hippocampus at the level of the anterior pons showing right lateralized atrophy of hippocampus in MCI and left lateralized atrophy of hippocampus in AD. e Unfolded view of the cerebellar cortex showing fissures and lobules from I to X depicting atrophy of lobule 1-4 and lobule 6 in vermis and paravermian region in MCI ; while in AD there is atrophy of lobule 1-4 and lobule 6 in vermis and paravermian region with extension to hemispheric involvement of lobule 6 and crux 1 of cerebellum. f Mid sagittal section showing white matter changes in corpus callosum with atrophy of genu and rostrum in MCI and atrophy of genu, rostrum and splenium in AD. g Axial section of brain at level of basal ganglia and midventricular levels showing areas of decreased FA in DTI studies involving left posterior limb of internal capsule (*green*), left thalamus (*yellow*), left caudate nucleus (*orange*), left anterior corona radiata (*red*) and bilateral posterior corona radiata (*purple*) in AD. h White matter tracts affected in MCI and AD: h1 Sagittal section showing uncinate fasciculus (*green*) and fornix (*purple*) in MCI h2 Sagittal sections showing uncinate fasciculus (*green*), fornix (*purple*), superior longitudinal fasciculus (*yellow*), inferior longitudinal fasciculus (*brown*), inferior fronto-occipital fasciculus (*red*) in AD.

degeneration, demyelination, cytoskeletal disorganization, packing density, and other microstructural features can affect the DTI measurements [42–44]. The summarized GM and WM changes in MCI and AD are depicted in Fig. 2.

A study combining VBM and DTI found a reduction in WM density in anterior CC, including genu and rostrum in PwMCI with no difference in FA, radial diffusivity (DR), and axial diffusivity (DA). In contrast, volume reduction in both anterior and posterior CC along with decreased

FA and DR in anterior CC, and increased DA in posterior CC regions were found in AD [38]. Abnormalities in DTI showed topographical differences. MCI-associated WM abnormality was reported in the left posterior cingulate, PHG, thalamus, caudate and bilateral precuneus by Gu and Zhang [26]. Sexton et al. observed that PwMCI had reduced FA in all WM regions except parietal and occipital areas and increased mean diffusivity (MD) in all except frontal and occipital regions. In contrast, PwAD had reduced FA in all regions except internal capsule and parietal WM with increased MD in all regions [45]. Furthermore, in MCI, FA and MD changes had larger effect size (ES) in parahippocampal cingulum (PHC) and HIP, respectively. Similarly, in AD, FA had larger ES in the total cingulum and PHC, splenium of CC, and uncinate fasciculus, while MD had larger ES in the HIP, parietal lobe, splenium of CC, and temporal lobe [35].

Additionally, another multimodal study of VBM and DTI in AD observed WM reductions in bilateral inferior temporal gyrus, splenium of CC, right PHG and HIP. WM volume reduction in bilateral PHG was associated with a higher mini-mental state examination (MMSE) score while affection of right HIP and splenium of CC was observed with a lower score [8]. In contrast to the meta-analysis by Sexton et al. in which the internal capsule was not found to be affected by FA changes, this study showed decreased FA values in the left posterior limb of internal capsule (PLIC), which contains pyramidal tract that connects cerebral cortex to the brainstem and spinal cord, left anterior corona radiata associated with motor and cognitive functions, left thalamus and left caudate nucleus in PwAD. Furthermore, significant WMV and FA reduction was identified in the left caudate nucleus, left corona radiata and right inferior temporal gyrus (traversed by uncinate fasciculus and fornix) [8]. Uncinate fasciculus, with its connections to the frontal lobe, insula, and rostral part of the temporal lobe, fornix, which is connected to other limbic structures via Papez circuit along with HIP and PHG, form essential components of a memory circuit [8, 34]. The damage to uncinate fasciculus and fornix seen in AD thus manifests clinically as memory impairment. Superior longitudinal fasciculus (SLF) arising from the prefrontal lobe, connecting frontal, parietal and occipital lobes and ending at temporal lobe was another noteworthy but less significant structure that showed a reduction in both WMV and FA values in AD [8]. In addition to CC, DWI and DTI studies have found damage to inferior fronto-occipital fasciculus and inferior longitudinal fasciculus, which functionally contribute to comprehension of meaningful speech and auditory perceptions, respectively [34]. Consistent WM alterations were seen as reduced FA in fornix and UF with increased MD in genu and splenium of CC, UF, and PHC. The MD changes, which displayed more considerable differences and less heterogeneity, were more dependable than FA. Alteration of the fornix, UF, and PHC served as a sensitive marker for reliably depicting amnestic MCI (aMCI) and tracking disease progression. Whole-brain ALE meta-analysis revealed a reduction in FA in bilateral posterior corona radiata, thus implicating its role in memory impairment. Both ROI-based and whole-brain-based research were found to be complementary to each other to obtain a complete picture of associated WM microstructural alterations [46].

Comparative evaluation of MTL volumetry and DTI revealed that volumetric measurements are more effective than DTI measurements; however, in PwMCI, increased MD of the HIP was a more sensitive indicator than HIP volume. Increased MD in the left HIP region was the strongest predictor of poor verbal and memory performance, while the HIP volume explained low variability in memory function. DTI measurements showed more overlap in MCI and AD as against MTL volumetry which could be explained by the fact that alterations in WM integrity precede the atrophic changes [35].

Neural Correlates from fMRI in MCI and AD

Both MCI and AD are characterized by widespread neuronal degeneration, and loss of connectivity among brain regions affecting neural pathways and disrupting the functional coherence of brain activities. The MCI and AD show abnormal regional brain activation as well as large-scale neuronal network dysfunctions. Multiple large-scale dysfunctional neuronal networks may be responsible for AD-associated cognitive impairment [47]. Functional MRI has been used to examine the alterations in functional connectivity of brain regions in AD and MCI. The structural atrophy correlates with the specific cognitive functions in MCI and AD, based on fMRI findings, are depicted in Fig. 3.

In a large study involving 1000 healthy controls (HC) and rs-fMRI, Yeo et al. identified seven cortical neuronal networks: the visual, somatomotor, dorsal attention, ventral attention, limbic, frontoparietal, and DMN [48]. The DMN is a network that involves the medial prefrontal cortex (PFC), PCC, precuneus, anterior cingulate cortex, parietal cortex, and the MTL, including the HIP [49, 50]. Furthermore, the authors parcellated the cerebellum and striatum into these seven networks based on the functional connectivity findings [51, 52].

In aMCI, atypical regional spontaneous brain activity, predominantly involving the default mode, salience (which consists of the anterior insula, dorsal anterior cingulate cortex), and visual cortical networks (middle occipital gyrus, lingual gyrus, inferior temporal gyrus, and calcarine cortex) has been reported [53, 54]. The decreased activation was mainly detected in frontoparietal and default networks in MCI, whereas AD patients showed more hypoactiva-

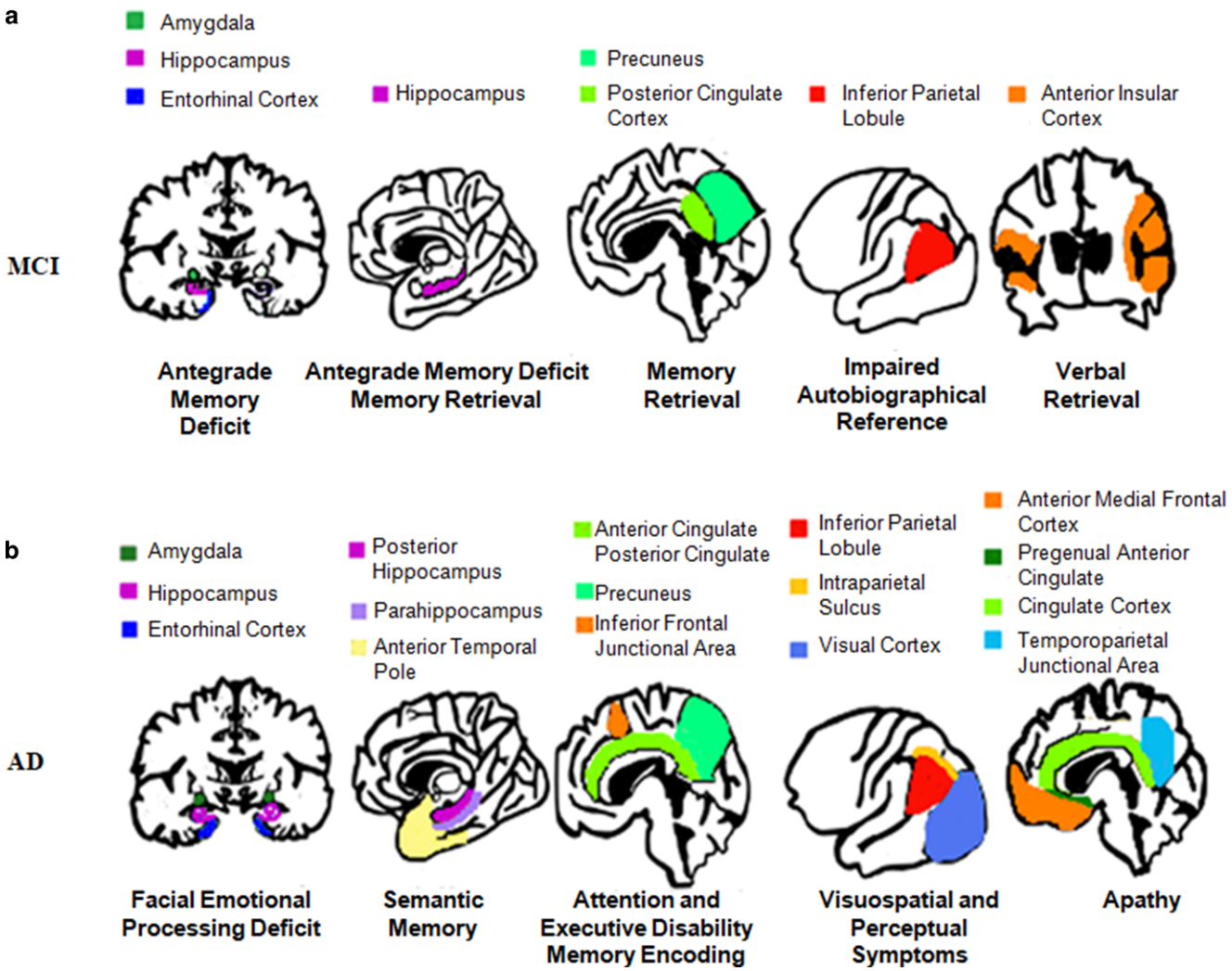

Fig. 3 Schematic representation of inferences from the various meta-analytical studies. The figure shows the structural atrophy correlates with the specific cognitive functions in **a** MCI and **b** AD. The disease begins in the medial temporal lobe mainly the entorhinal cortex, hippocampus consistent with symptoms of memory impairment. Coronal sections depict the structural atrophy correlates of antegrade memory deficit, verbal retrieval and facial emotional processing deficit while sagittal sections show the progression of degeneration to the lateral temporal and parietal lobe, accompanying language and visuospatial dysfunction and the basal forebrain degeneration that occurs with abnormal behavior manifestation

tion voxels in the visual network. Similarly, frontoparietal, ventral attention, somatomotor, and default networks were involved in the compensatory process in both MCI and AD [55]. Although DMN functional connectivity is inconsistent, reduced PCC connectivity in MCI could prove to be a potential biomarker of risk for developing AD [56].

A meta-analysis by Wang et al. presented a consistent pattern of DMN disruption in PwaMCI, specifically involving reduced functional connectivity in the bilateral precuneus/PCC and MTL. Furthermore, DMN functional connectivity in the bilateral medial prefrontal cortices (including the ACC), bilateral angular gyri extending to the middle temporal gyri, and right temporal pole extending to the middle temporal gyrus (MTG) positively correlated with the severity of global cognitive impairment (MMSE scores), likely reflecting a compensatory mechanism for maintaining cognitive efficiency [57].

Consistent alterations in connectivity were found in the DMN, SN, and limbic networks in PwAD, MCI, or in both groups. With the anterior insula as a key hub, the SN plays a pivotal role in network switching between the DMN and frontoparietal network (FPN), two networks exhibiting competitive interactions during cognitive information processing. Association of heightened SN connectivity with reduced DMN connectivity in AD suggests that progressive DMN impairment may be deleterious to SN function [58].

The MCI-associated resting state hypoactivation has been observed in the left superior temporal gyrus (STG), right posterior cingulate/precuneus, uncus while increased activation in the inferior parietal lobule, superior parietal

lobule compared to HC [26]. Furthermore, in aMCI, apart from MTG, reduced resting state activity was also observed in the PCC, right angular gyrus, right PHG and left fusiform gyrus. Reduced resting state activity in the PCC has been demonstrated as being unique to aMCI patients compared to other subtypes such as subcortical vascular MCI (svMCI). Interestingly, the hypoactivation in the PCC was found to be independent of the GM volume alterations; however, hyperactivation in the left MTG and left supramarginal gyrus appears to be a compensatory response or indicates other pathological changes, such as excitotoxicity that triggers neuronal apoptosis [59].

Task-related fMRI meta-analysis indicated that MCI is associated with reduced activity in the left inferior parietal lobule, right posterior cingulate, and bilateral precuneus whereas hyperactivation in the left middle frontal gyrus, superior parietal lobule, insula, STG, and right inferior frontal gyrus [26]. The MTL activity deficits across encoding and retrieval paradigms are consistent in PwAD when compared to HC; however, mildly affected patients show consistently preserved right hemisphere MTL activity during encoding. Furthermore, patients showed consistently greater activity in the dorsolateral prefrontal cortex (DL-PFC) and ventrolateral prefrontal cortex (VL-PFC) during encoding and retrieval tasks when compared to HC. In contrast, HC showed greater rostrolateral PFC (RL-PFC) involvement during both processes. It is suggested that the pattern of differential prefrontal involvement reflects compensatory changes occurring in AD [60].

Disease stage-dependent brain activation pattern related to the pathognomonic AD characteristic of episodic memory loss exists. Early memory encoding task-related right HIP hyperactivation (mainly CA2-4 subregions) in PwMCI and within the precuneus in PwAD is followed by retrieval task-related decreased activation in the left HIP (especially in the CA1, subiculum and PHG) and fusiform gyrus in PwMCI and right HIP in PwAD [61].

In the meta-analysis by Terry et al. hyperactivation was reported in MTL, frontal, and occipitotemporal lobes in healthy older adults, but lesser and no MTL activation was found in AD and MCI along with the absence of cortical involvement as compared to HC [62]. Interestingly, the bilateral angular and the middle temporal cortex, or superior frontal gyri, have been demonstrated as the primary target for DMN modulation using non-invasive brain stimulation in AD [63].

Neural Correlates from PET in MCI and AD

Molecular imaging with PET has emerged as a neuroimaging modality with significant potential for early diagnosis, assessing disease progression, subtype characterization, and management of AD and MCI [64, 65]. Using PET radiotracers can provide important clinical information, e.g. (18F) FDG as a biomarker of neuronal degeneration or Aβ/tau PET as a biomarker of AD neuropathology [66].

Specifically, the inferior parietal lobules (IPL) and precuneus were found to be functionally involved in early AD. The findings suggest that hypometabolism/hypoperfusion in the IPL most reliably predicts the progression from aMCI to AD [21]. Regional hypometabolism in the left PCC/precuneus at baseline was able to accurately differentiate between aMCI converters from non-converters [67]. Interestingly, FDG-PET has been shown to perform slightly better than structural MRI and single-photon emission computed tomography (SPECT) in predicting conversion to AD in PwMCI [68].

The Pittsburgh compound B (PiB) PET scan show aggregated fibrillar amyloid accumulation in vivo. Currently, there are three FDA-approved 18F Aβ PET radiotracers used in clinical practice for diagnosis of AD: florbetaben (Neuraceq™, Piramal Imaging, Boston, MA, USA), florbetapir (Amyvid™, Eli Lilly, Indianapolis, IN, USA), and flutemetamol (18F) (Vizamyl™, GE Healthcare, Medi-Physics, Inc., Arlington Heights, IL, USA) [69]. Although a meta-analysis by Morris et al. assessing the diagnostic accuracy of the three Aβ radiotracers revealed no marked differences, Yeo et al. demonstrated a higher sensitivity, similar/comparable specificity, and a higher OR for florbetapir as compared to florbetaben in differentiating AD patients from HC [70, 71].

The prevalence of amyloid positivity on PET has been shown to vary with age and *APOE* status among AD and other dementias. It decreased with age in PwAD (most significant in *APOE*4 non-carriers) and increased with age in other non-AD dementia subtypes. Furthermore, negative amyloid positivity was seen in 12% of clinically diagnosed PwAD and was most common in older *APOE*4 non-carriers [72]. Although higher age-specific amyloid positivity rates have been reported with the highest in >80 years (65%) to 37% in 70–79 years of age group and 18% in 60–69 years age range [73], Chen et al. reported that positive PiB increases risks for conversion to AD by 3.7 times with mean follow-up duration ranging from 1 to 3.8 years. Baseline positive PiB was also shown to predict conversion from MCI to AD [74]. Compared with ^{18}F-FDG PET and structural MRI, ^{11}C-PiB-PET achieved higher sensitivity but relatively lower specificity in the early diagnosis of AD from MCI with short-term follow-up; however, increase in follow-up duration resulted in higher accuracy of ^{11}C-PiB-PET for predicting progression to AD among PwMCI [74].

In an interesting meta-analysis, increased neuroinflammation was found to be associated with the progression of MCI and AD, relative to HCs. The authors found increased translocator protein (TSPO) levels in PwAD and PwMCI, mainly in frontotemporal regions and neocortex compared

to HC, respectively [75]. Their findings provide support to the dual hit inflammatory hypothesis in MCI/AD development and progression. The role of inflammation as an initial event in the MCI/AD pathogenesis has been gaining support and has also been proposed by the systemic immune dyshomeostasis model hypothesis [76].

Neural Correlates from MRS in MCI and AD

Using MRS monitors changes in brain metabolites occurring in early degeneration and is therefore implicated as a biochemical neuroimaging marker in AD. In aMCI, PC, HIP, and paratrigonal white matter (PWM) were brain areas of interest for MRS changes. Raised myoinositol (mI) concentration and choline/creatine ratio (Cho/Cr), along with reduced N-acetyl aspartate (NAA) level and NAA/mI ratio, was observed in the PC. HIP showed reduced NAA, creatine, and choline with raised mI/Cr ratio consistently, while PWM showed a reduction in NAA and creatine. NAA was found to be the most reliable marker of brain dysfunction in MCI [77].

Another study confirmed that in AD, absolute NAA concentration was reduced in PC and HIP. The role of NAA in neuroenergetics is assumed because it is produced in the mitochondria and a regional decrease indicates diminished neuronal density, neuronal cell loss or partially reversible neuronal dysfunction [78, 79]. In addition, NAA/Cr ratio is reduced in PC, parietal WM, parietal GM and temporal lobe. In comparison, a prior study observed that mI/Cr ratio was much higher in PwAD and mI changes preceding NAA changes [80]. Wang et al. observed an increase in the absolute concentration of mI in PC with an increased mI/Cr ratio in parietal GM. They concluded that NAA/Cr was a reliable parameter to differentiate AD from HC, and changes in NAA supplement the diagnostic accuracy [81]. The findings from MRS are summarized in Table S2.

Limitations

Both clinical and experimental heterogeneity were observed in the selection of included studies from 46 meta-analysis studies. For instance, in several meta-analysis studies, different diagnostic criteria were used by included studies probably as there are different guidelines for the diagnosis of AD and some have been updated in the past few years. Most of the included studies have used one of the following internationally recognized diagnostic criteria for: MCI: (1) Petersen criteria (1999, 2001, 2004, 2005, 2011) [82–86], (2) Winblad (2004) [6], (3) National Institute on Aging—Alzheimer's Association Workgroup MCI due to AD criteria (NIA-AA) [87], (4) ADNI early and late MCI criteria [88] and AD (1) NINCDS-ADRDA [89], (2) DSM-IIIR Diagnostic and Statistical Manual of Mental Disorders (DSM) third edition or DSM-IV [90], (4) International Classification of Diseases (ICD)-10 [91], (5) clinical dementia rating [92], (6) National Institute on Aging (NIA)—Reagan Institute [93]. The diagnoses in majority of the papers were made clinically without using CSF or amyloid PET biomarker information.

During the study selection for the present systematic review, no distinction between possible and probable AD and MCI subtypes including the severity stages was made. All meta-analyses articles have included studies using different MRI magnetic field strengths (range: 0.5–4T), which could have attributed to heterogeneity. These additional characteristics of included studies in the systematic review are provided in Table S3. We did not exclude meta-analysis studies based on the quality but rather examined various aspects of the studies in order to summarize their relationship to the findings.

Conclusion

The advanced multimodality anatomic and molecular imaging approaches have shown substantial utility in the early diagnosis of AD and assessing the progression of MCI to AD. Specialized computerized software has aided in automatic volumetric analysis and quantitative assessment of specific brain regions associated with the disease specific anatomic, functional, and pathological features. Anatomically, hippocampal atrophy has emerged as a potential MCI/AD biomarker. Although the findings on the eventual use of resting state or task-based fMRI as an imaging biomarker are promising, no index of default mode network connectivity qualifies as a valuable biomarker of MCI or risk for AD. The presence of risk factors such as HIP, MTL and EC atrophy, *APOEε4*, altered WM integrity, increased amyloid deposition and reduced cerebral metabolism had the strongest positive association for MCI to AD progression. The identified brain regions involved in pathological and compensatory mechanisms need to be confirmed in future studies. Furthermore, future quantitative studies should consider uniform study design with analytical pipelines for reproducibility of results and to conduct robust meta-analyses. Investigating the underlying AD pathology through the combination of multimodal imaging and extensive neurocognitive assessment may help in early diagnosis, differential diagnosis, planning management strategies, and facilitating personalized medicine.

Supplementary Information The online version of this article (https://doi.org/10.1007/s00062-021-01057-7) contains supplementary material, which is available to authorized users.

Acknowledgements We thank the Director, Nimesh G Desai, Institute of Human Behaviour and Allied Sciences (IHBAS), for motivation and unconditional support. PT acknowledges DST, Government of India for providing fellowship (CSRI-PDF). We thank the anonymous reviewers for their helpful suggestions for improving the manuscript.

Funding This research did not receive any specific grant from funding agencies in the public, commercial, or not-for-profit sectors.

Author Contribution P. Talwar and S. Kushwaha conceived, performed data mining, interpretation, and wrote the study. M. Chaturvedi performed literature mining, data interpretation and wrote the manuscript. V. Mahajan contributed by helping in improving the manuscript. All the authors read and approved the final manuscript.

Declarations

Conflict of interest P. Talwar, S. Kushwaha, M. Chaturvedi and V. Mahajan declare that they have no competing interests.

Ethical standards For this article no studies with human participants or animals were performed by any of the authors.

References

1. Patterson C. World Alzheimer report 2018—the state of the art of dementia research: new frontiers. London, UK: Alzheimer's Disease International (ADI); 2018.
2. WHO. Dementia. 2019. https://www.who.int/news-room/fact-sheets/detail/dementia. Accessed 8 Aug 2019.
3. Frisoni GB, Weiner MW. Alzheimer's Disease Neuroimaging Initiative special issue. Neurobiol Aging. 2010;31:1259–62.
4. Braak H, Braak E. Demonstration of amyloid deposits and neurofibrillary changes in whole brain sections. Brain Pathol. 1991;1:213–6.
5. Petersen RC. Mild cognitive impairment: transition between aging and Alzheimer's disease. Neurologia. 2000;15:93–101.
6. Winblad B, Palmer K, Kivipelto M, Jelic V, Fratiglioni L, Wahlund LO, Nordberg A, Bäckman L, Albert M, Almkvist O, Arai H, Basun H, Blennow K, de Leon M, DeCarli C, Erkinjuntti T, Giacobini E, Graff C, Hardy J, Jack C, Jorm A, Ritchie K, van Duijn C, Visser P, Petersen RC. Mild cognitive impairment--beyond controversies, towards a consensus: report of the International Working Group on Mild Cognitive Impairment. J Intern Med. 2004;256:240–6.
7. Le Bihan D, Turner R, Douek P, Patronas N. Diffusion MR imaging: clinical applications. AJR Am J Roentgenol. 1992;159:591–9.
8. Yin RH, Tan L, Liu Y, Wang WY, Wang HF, Jiang T, Radua J, Zhang Y, Gao J, Canu E, Migliaccio R, Filippi M, Gorno-Tempini ML, Yu JT. Multimodal Voxel-Based Meta-Analysis of White Matter Abnormalities in Alzheimer's Disease. J Alzheimers Dis. 2015;47:495–507.
9. Fan J, Donkin J, Wellington C. Greasing the wheels of Abeta clearance in Alzheimer's disease: the role of lipids and apolipoprotein E. Biofactors. 2009;35:239–48.
10. Lerch JP, Pruessner J, Zijdenbos AP, Collins DL, Teipel SJ, Hampel H, Evans AC. Automated cortical thickness measurements from MRI can accurately separate Alzheimer's patients from normal elderly controls. Neurobiol Aging. 2008;29:23–30.
11. Vemuri P, Gunter JL, Senjem ML, Whitwell JL, Kantarci K, Knopman DS, Boeve BF, Petersen RC, Jack CR Jr. Alzheimer's disease diagnosis in individual subjects using structural MR images: validation studies. Neuroimage. 2008;39:1186–97.
12. Julkunen V, Niskanen E, Koikkalainen J, Herukka SK, Pihlajamäki M, Hallikainen M, Kivipelto M, Muehlboeck S, Evans AC, Vanninen R, Hilkka Soininen. Differences in cortical thickness in healthy controls, subjects with mild cognitive impairment, and Alzheimer's disease patients: a longitudinal study. J Alzheimers Dis. 2010;21:1141–51.
13. Koch K, Myers NE, Göttler J, Pasquini L, Grimmer T, Förster S, Manoliu A, Neitzel J, Kurz A, Förstl H, Riedl V, Wohlschläger AM, Drzezga A, Sorg C. Disrupted Intrinsic Networks Link Amyloid-β Pathology and Impaired Cognition in Prodromal Alzheimer's Disease. Cereb Cortex. 2015;25:4678–88.
14. Fox MD, Snyder AZ, Vincent JL, Corbetta M, Van Essen DC, Raichle ME. The human brain is intrinsically organized into dynamic, anticorrelated functional networks. Proc Natl Acad Sci U S A. 2005;102:9673–8.
15. van den Heuvel MP, Mandl RC, Kahn RS, Hulshoff Pol HE. Functionally linked resting-state networks reflect the underlying structural connectivity architecture of the human brain. Hum Brain Mapp. 2009;30:3127–41.
16. Zhang XY, Yang ZL, Lu GM, Yang GF, Zhang LJ. PET/MR Imaging: New Frontier in Alzheimer's Disease and Other Dementias. Front Mol Neurosci. 2017;10:343.
17. Ishii K. PET approaches for diagnosis of dementia. AJNR Am J Neuroradiol. 2014;35:2030–8.
18. Murray ME, Przybelski SA, Lesnick TG, Liesinger AM, Spychalla A, Zhang B, Gunter JL, Parisi JE, Boeve BF, Knopman DS, Petersen RC, Jack CR Jr, Dickson DW, Kantarci K. Early Alzheimer's disease neuropathology detected by proton MR spectroscopy. J Neurosci. 2014;34:16247–55.
19. Ashburner J, Friston KJ. Voxel-based morphometry--the methods. Neuroimage. 2000;11:805–21.
20. Giorgio A, De Stefano N. Clinical use of brain volumetry. J Magn Reson Imaging. 2013;37:1–14.
21. Schroeter ML, Stein T, Maslowski N, Neumann J. Neural correlates of Alzheimer's disease and mild cognitive impairment: a systematic and quantitative meta-analysis involving 1351 patients. Neuroimage. 2009;47:1196–206.
22. Rathakrishnan BG, Doraiswamy PM, Petrella JR. Science to practice: translating automated brain MRI volumetry in Alzheimer's disease from research to routine diagnostic use in the work-up of dementia. Front Neurol. 2014;4:216.
23. Manuello J, Nani A, Premi E, Borroni B, Costa T, Tatu K, Liloia D, Duca S, Cauda F. The Pathoconnectivity Profile of Alzheimer's Disease: A Morphometric Coalteration Network Analysis. Front Neurol. 2018;8:739.
24. Zakzanis KK, Graham SJ, Campbell Z. A meta-analysis of structural and functional brain imaging in dementia of the Alzheimer's type: a neuroimaging profile. Neuropsychol Rev. 2003;13:1–18.
25. Yang J, Pan P, Song W, Huang R, Li J, Chen K, Gong Q, Zhong J, Shi H, Shang H. Voxelwise meta-analysis of gray matter anomalies in Alzheimer's disease and mild cognitive impairment using anatomic likelihood estimation. J Neurol Sci. 2012;316:21–9.
26. Gu L, Zhang Z. Exploring Structural and Functional Brain Changes in Mild Cognitive Impairment: A Whole Brain ALE Meta-Analysis for Multimodal MRI. ACS Chem Neurosci. 2019;10:2823–9.
27. Fathy YY, Hoogers SE, Berendse HW, van der Werf YD, Visser PJ, de Jong FJ, van de Berg WDJ. Differential insular cortex subregional atrophy in neurodegenerative diseases: a systematic review and meta-analysis. Brain Imaging Behav. 2020;14:2799–816.
28. Schroeter ML, Neumann J. Combined Imaging Markers Dissociate Alzheimer's Disease and Frontotemporal Lobar Degeneration - An ALE Meta-Analysis. Front Aging Neurosci. 2011;3:10.
29. Chapleau M, Aldebert J, Montembeault M, Brambati SM. Atrophy in Alzheimer's Disease and Semantic Dementia: An ALE Meta-Analysis of Voxel-Based Morphometry Studies. J Alzheimers Dis. 2016;54:941–55.

30. Wang WY, Yu JT, Liu Y, Yin RH, Wang HF, Wang J, Tan L, Radua J, Tan L. Voxel-based meta-analysis of grey matter changes in Alzheimer's disease. Transl Neurodegener. 2015;4:6.
31. Barnes J, Bartlett JW, van de Pol LA, Loy CT, Scahill RI, Frost C, Thompson P, Fox NC. A meta-analysis of hippocampal atrophy rates in Alzheimer's disease. Neurobiol Aging. 2009;30:1711–23.
32. Tabatabaei-Jafari H, Shaw ME, Cherbuin N. Cerebral atrophy in mild cognitive impairment: A systematic review with meta-analysis. Alzheimers Dement (Amst). 2015;1:487–504.
33. Minkova L, Habich A, Peter J, Kaller CP, Eickhoff SB, Klöppel S. Gray matter asymmetries in aging and neurodegeneration: A review and meta-analysis. Hum Brain Mapp. 2017;38:5890–904.
34. Li J, Pan P, Huang R, Shang H. A meta-analysis of voxel-based morphometry studies of white matter volume alterations in Alzheimer's disease. Neurosci Biobehav Rev. 2012;36:757–63.
35. Clerx L, Visser PJ, Verhey F, Aalten P. New MRI markers for Alzheimer's disease: a meta-analysis of diffusion tensor imaging and a comparison with medial temporal lobe measurements. J Alzheimers Dis. 2012;29:405–29.
36. Gellersen HM, Guo CC, O'Callaghan C, Tan RH, Sami S, Hornberger M. Cerebellar atrophy in neurodegeneration-a meta-analysis. J Neurol Neurosurg Psychiatry. 2017;88:780–8.
37. Schulte T, Müller-Oehring EM. Contribution of callosal connections to the interhemispheric integration of visuomotor and cognitive processes. Neuropsychol Rev. 2010;20:174–90.
38. Wang XD, Ren M, Zhu MW, Gao WP, Zhang J, Shen H, Lin ZG, Feng HL, Zhao CJ, Gao K. Corpus callosum atrophy associated with the degree of cognitive decline in patients with Alzheimer's dementia or mild cognitive impairment: a meta-analysis of the region of interest structural imaging studies. J Psychiatr Res. 2015;63:10–9.
39. Di Paola M, Luders E, Di Iulio F, Cherubini A, Passafiume D, Thompson PM, Caltagirone C, Toga AW, Spalletta G. Callosal atrophy in mild cognitive impairment and Alzheimer's disease: different effects in different stages. Neuroimage. 2010;49:141–9.
40. Ferreira LK, Diniz BS, Forlenza OV, Busatto GF, Zanetti MV. Neurostructural predictors of Alzheimer's disease: a meta-analysis of VBM studies. Neurobiol Aging. 2011;32:1733–41.
41. Seo EH, Park WY, Choo IH. Structural MRI and Amyloid PET Imaging for Prediction of Conversion to Alzheimer's Disease in Patients with Mild Cognitive Impairment: A Meta-Analysis. Psychiatry Investig. 2017;14:205–15.
42. Taylor WD, Hsu E, Krishnan KR, MacFall JR. Diffusion tensor imaging: background, potential, and utility in psychiatric research. Biol Psychiatry. 2004;55:201–7.
43. Soares JM, Marques P, Alves V, Sousa N. A hitchhiker's guide to diffusion tensor imaging. Front Neurosci. 2013;7:31.
44. Alexander AL, Lee JE, Lazar M, Field AS. Diffusion tensor imaging of the brain. Neurotherapeutics. 2007;4:316–29.
45. Sexton CE, Kalu UG, Filippini N, Mackay CE, Ebmeier KP. A meta-analysis of diffusion tensor imaging in mild cognitive impairment and Alzheimer's disease. Neurobiol Aging. 2011;32:2322.e5-18.
46. Yu J, Lam CLM, Lee TMC. White matter microstructural abnormalities in amnestic mild cognitive impairment: A meta-analysis of whole-brain and ROI-based studies. Neurosci Biobehav Rev. 2017;83:405–16.
47. Dickerson BC, Sperling RA. Large-scale functional brain network abnormalities in Alzheimer's disease: insights from functional neuroimaging. Behav Neurol. 2009;21:63–75.
48. Yeo BT, Krienen FM, Sepulcre J, Sabuncu MR, Lashkari D, Hollinshead M, Roffman JL, Smoller JW, Zöllei L, Polimeni JR, Fischl B, Liu H, Buckner RL. The organization of the human cerebral cortex estimated by intrinsic functional connectivity. J Neurophysiol. 2011;106:1125–65.
49. Greicius MD, Menon V. Default-mode activity during a passive sensory task: uncoupled from deactivation but impacting activation. J Cogn Neurosci. 2004;16:1484–92.
50. Buckner RL, Andrews-Hanna JR, Schacter DL. The brain's default network: anatomy, function, and relevance to disease. Ann N Y Acad Sci. 2008;1124:1–38.
51. Buckner RL, Krienen FM, Castellanos A, Diaz JC, Yeo BT. The organization of the human cerebellum estimated by intrinsic functional connectivity. J Neurophysiol. 2011;106:2322–45.
52. Choi EY, Yeo BT, Buckner RL. The organization of the human striatum estimated by intrinsic functional connectivity. J Neurophysiol. 2012;108:2242–63.
53. Pan P, Zhu L, Yu T, Shi H, Zhang B, Qin R, Zhu X, Qian L, Zhao H, Zhou H, Xu Y. Aberrant spontaneous low-frequency brain activity in amnestic mild cognitive impairment: A meta-analysis of resting-state fMRI studies. Ageing Res Rev. 2017;35:12–21.
54. Allen EA, Erhardt EB, Damaraju E, Gruner W, Segall JM, Silva RF, Havlicek M, Rachakonda S, Fries J, Kalyanam R, Michael AM, Caprihan A, Turner JA, Eichele T, Adelsheim S, Bryan AD, Bustillo J, Clark VP, Feldstein Ewing SW, Filbey F, Ford CC, Hutchison K, Jung RE, Kiehl KA, Kodituwakku P, Komesu YM, Mayer AR, Pearlson GD, Phillips JP, Sadek JR, Stevens M, Teuscher U, Thoma RJ, Calhoun VD. A baseline for the multivariate comparison of resting-state networks. Front Syst Neurosci. 2011;5:2.
55. Li HJ, Hou XH, Liu HH, Yue CL, He Y, Zuo XN. Toward systems neuroscience in mild cognitive impairment and Alzheimer's disease: a meta-analysis of 75 fMRI studies. Hum Brain Mapp. 2015;36:1217–32.
56. Eyler LT, Elman JA, Hatton SN, Gough S, Mischel AK, Hagler DJ, Franz CE, Docherty A, Fennema-Notestine C, Gillespie N, Gustavson D, Lyons MJ, Neale MC, Panizzon MS, Dale AM, Kremen WS. Resting State Abnormalities of the Default Mode Network in Mild Cognitive Impairment: A Systematic Review and Meta-Analysis. J Alzheimers Dis. 2019;70:107–20.
57. Wang C, Pan Y, Liu Y, Xu K, Hao L, Huang F, Ke J, Sheng L, Ma H, Guo W. Aberrant default mode network in amnestic mild cognitive impairment: a meta-analysis of independent component analysis studies. Neurol Sci. 2018;39:919–31.
58. Badhwar A, Tam A, Dansereau C, Orban P, Hoffstaedter F, Bellec P. Resting-state network dysfunction in Alzheimer's disease: A systematic review and meta-analysis. Alzheimers Dement (Amst). 2017;8:73–85.
59. Lau WK, Leung MK, Lee TM, Law AC. Resting-state abnormalities in amnestic mild cognitive impairment: a meta-analysis. Transl Psychiatry. 2016;6:e790.
60. Schwindt GC, Black SE. Functional imaging studies of episodic memory in Alzheimer's disease: a quantitative meta-analysis. Neuroimage. 2009;45:181–90.
61. Nellessen N, Rottschy C, Eickhoff SB, Ketteler ST, Kuhn H, Shah NJ, Schulz JB, Reske M, Reetz K. Specific and disease stage-dependent episodic memory-related brain activation patterns in Alzheimer's disease: a coordinate-based meta-analysis. Brain Struct Funct. 2015;220:1555–71.
62. Terry DP, Sabatinelli D, Puente AN, Lazar NA, Miller LS. A Meta-Analysis of fMRI Activation Differences during Episodic Memory in Alzheimer's Disease and Mild Cognitive Impairment. J Neuroimaging. 2015;25:849–60.
63. Pievani M, Pini L, Ferrari C, Pizzini FB, Boscolo Galazzo I, Cobelli C, Cotelli M, Manenti R, Frisoni GB. Coordinate-Based Meta-Analysis of the Default Mode and Salience Network for Target Identification in Non-Invasive Brain Stimulation of Alzheimer's Disease and Behavioral Variant Frontotemporal Dementia Networks. J Alzheimers Dis. 2017;57:825–43.
64. Chandra A, Valkimadi PE, Pagano G, Cousins O, Dervenoulas G, Politis M; Alzheimer's Disease Neuroimaging Initiative. Applications of amyloid, tau, and neuroinflammation PET imaging to

Alzheimer's disease and mild cognitive impairment. Hum Brain Mapp. 2019;40:5424–42.
65. Matsuda H, Shigemoto Y, Sato N. Neuroimaging of Alzheimer's disease: focus on amyloid and tau PET. Jpn J Radiol. 2019;37:735–49.
66. Barthel H, Schroeter ML, Hoffmann KT, Sabri O. PET/MR in dementia and other neurodegenerative diseases. Semin Nucl Med. 2015;45:224–33.
67. Ma HR, Sheng LQ, Pan PL, Wang GD, Luo R, Shi HC, Dai ZY, Zhong JG. Cerebral glucose metabolic prediction from amnestic mild cognitive impairment to Alzheimer's dementia: a meta-analysis. Transl Neurodegener. 2018;7:9.
68. Yuan Y, Gu ZX, Wei WS. Fluorodeoxyglucose-positron-emission tomography, single-photon emission tomography, and structural MR imaging for prediction of rapid conversion to Alzheimer disease in patients with mild cognitive impairment: a meta-analysis. AJNR Am J Neuroradiol. 2009;30:404–10.
69. Choe YS, Lee KH. PET Radioligands for Imaging of Tau Pathology: Current Status. Nucl Med Mol Imaging. 2015;49:251–7.
70. Morris E, Chalkidou A, Hammers A, Peacock J, Summers J, Keevil S. Diagnostic accuracy of (18)F amyloid PET tracers for the diagnosis of Alzheimer's disease: a systematic review and meta-analysis. Eur J Nucl Med Mol Imaging. 2016;43:374–85.
71. Yeo JM, Waddell B, Khan Z, Pal S. A systematic review and meta-analysis of (18)F-labeled amyloid imaging in Alzheimer's disease. Alzheimers Dement (Amst). 2015;1:5–13.
72. Ossenkoppele R, Jansen WJ, Rabinovici GD, Knol DL, van der Flier WM, van Berckel BN, Scheltens P, Visser PJ; Amyloid PET Study Group, Verfaillie SC, Zwan MD, Adriaanse SM, Lammertsma AA, Barkhof F, Jagust WJ, Miller BL, Rosen HJ, Landau SM, Villemagne VL, Rowe CC, Lee DY, Na DL, Seo SW, Sarazin M, Roe CM, Sabri O, Barthel H, Koglin N, Hodges J, Leyton CE, Vandenberghe R, van Laere K, Drzezga A, Forster S, Grimmer T, Sánchez-Juan P, Carril JM, Mok V, Camus V, Klunk WE, Cohen AD, Meyer PT, Hellwig S, Newberg A, Frederiksen KS, Fleisher AS, Mintun MA, Wolk DA, Nordberg A, Rinne JO, Chételat G, Lleo A, Blesa R, Fortea J, Madsen K, Rodrigue KM, Brooks DJ. Prevalence of amyloid PET positivity in dementia syndromes: a meta-analysis. JAMA. 2015;313:1939–49.
73. Rowe CC, Ellis KA, Rimajova M, Bourgeat P, Pike KE, Jones G, Fripp J, Tochon-Danguy H, Morandeau L, O'Keefe G, Price R, Raniga P, Robins P, Acosta O, Lenzo N, Szoeke C, Salvado O, Head R, Martins R, Masters CL, Ames D, Villemagne VL. Amyloid imaging results from the Australian Imaging, Biomarkers and Lifestyle (AIBL) study of aging. Neurobiol Aging. 2010;31:1275–83.
74. Chen X, Li M, Wang S, Zhu H, Xiong Y, Liu X. Pittsburgh compound B retention and progression of cognitive status--a meta-analysis. Eur J Neurol. 2014;21:1060–7.
75. Bradburn S, Murgatroyd C, Ray N. Neuroinflammation in mild cognitive impairment and Alzheimer's disease: A meta-analysis. Ageing Res Rev. 2019;50:1–8.
76. Talwar P, Kushwaha S, Gupta R, Agarwal R. Systemic Immune Dyshomeostasis Model and Pathways in Alzheimer's Disease. Front Aging Neurosci. 2019;11:290.
77. Tumati S, Martens S, Aleman A. Magnetic resonance spectroscopy in mild cognitive impairment: systematic review and meta-analysis. Neurosci Biobehav Rev. 2013;37:2571–86.
78. Bates TE, Strangward M, Keelan J, Davey GP, Munro PM, Clark JB. Inhibition of N-acetylaspartate production: implications for 1H MRS studies in vivo. Neuroreport. 1996;7:1397–400.
79. Tsai G, Coyle JT. N-acetylaspartate in neuropsychiatric disorders. Prog Neurobiol. 1995;46:531–40.
80. Kantarci K, Knopman DS, Dickson DW, Parisi JE, Whitwell JL, Weigand SD, Josephs KA, Boeve BF, Petersen RC, Jack CR Jr. Alzheimer disease: postmortem neuropathologic correlates of antemortem 1H MR spectroscopy metabolite measurements. Radiology. 2008;248:210–20.
81. Wang H, Tan L, Wang HF, Liu Y, Yin RH, Wang WY, Chang XL, Jiang T, Yu JT. Magnetic Resonance Spectroscopy in Alzheimer's Disease: Systematic Review and Meta-Analysis. J Alzheimers Dis. 2015;46:1049–70.
82. Petersen RC, Smith GE, Waring SC, Ivnik RJ, Tangalos EG, Kokmen E. Mild cognitive impairment: clinical characterization and outcome. Arch Neurol. 1999;56:303–8. Erratum in: Arch Neurol 1999;56:760.
83. Petersen RC, Doody R, Kurz A, Mohs RC, Morris JC, Rabins PV, Ritchie K, Rossor M, Thal L, Winblad B. Current concepts in mild cognitive impairment. Arch Neurol. 2001;58:1985–92.
84. Petersen RC. Mild cognitive impairment as a diagnostic entity. J Intern Med. 2004;256:183–94.
85. Petersen RC, Morris JC. Mild cognitive impairment as a clinical entity and treatment target. Arch Neurol. 2005;62:1160–3; discussion 1167.
86. Petersen RC. Clinical practice. Mild cognitive impairment. N Engl J Med. 2011;364:2227–34.
87. Albert MS, DeKosky ST, Dickson D, Dubois B, Feldman HH, Fox NC, Gamst A, Holtzman DM, Jagust WJ, Petersen RC, Snyder PJ, Carrillo MC, Thies B, Phelps CH. The diagnosis of mild cognitive impairment due to Alzheimer's disease: recommendations from the National Institute on Aging-Alzheimer's Association workgroups on diagnostic guidelines for Alzheimer's disease. Alzheimers Dement. 2011;7:270–9.
88. Aisen PS, Petersen RC, Donohue MC, Gamst A, Raman R, Thomas RG, Walter S, Trojanowski JQ, Shaw LM, Beckett LA, Jack CR Jr, Jagust W, Toga AW, Saykin AJ, Morris JC, Green RC, Weiner MW; Alzheimer's Disease Neuroimaging Initiative. Clinical Core of the Alzheimer's Disease Neuroimaging Initiative: progress and plans. Alzheimers Dement. 2010;6:239–46.
89. McKhann G, Drachman D, Folstein M, Katzman R, Price D, Stadlan EM. Clinical diagnosis of Alzheimer's disease: report of the NINCDS-ADRDA work group under the auspices of department of health and human services task force on Alzheimer's disease. Neurology. 1984;34:939–44.
90. American Psychiatric Association. Diagnostic and statistical manual of mental disorders. 3rd ed. 1987. pp. 971–9.
91. World Health Organization. ICD-10: the ICD-10 classification of mental and behavioural disorders: diagnostic criteria for research. ICD-10: the ICD-10 classification of mental and behavioural disorders: diagnostic criteria for research. 1993. p. 248.
92. Morris JC. Clinical dementia rating: a reliable and valid diagnostic and staging measure for dementia of the Alzheimer type. Int Psychogeriatr. 1997;9 Suppl 1:173–6; discussion 177-8.
93. Newell KL, Hyman BT, Growdon JH, Hedley-Whyte ET. Application of the National Institute on Aging (NIA)-Reagan Institute criteria for the neuropathological diagnosis of Alzheimer disease. J Neuropathol Exp Neurol. 1999;58:1147–55.
94. Schmand B, Huizenga HM, van Gool WA. Meta-analysis of CSF and MRI biomarkers for detecting preclinical Alzheimer's disease. Psychol Med. 2010;40:135–45.
95. Boccia M, Acierno M, Piccardi L. Neuroanatomy of Alzheimer's Disease and Late-Life Depression: A Coordinate-Based Meta-Analysis of MRI Studies. J Alzheimers Dis. 2015;46:963–70.
96. Liu Y, Yu JT, Wang HF, Han PR, Tan CC, Wang C, Meng XF, Risacher SL, Saykin AJ, Tan L. APOE genotype and neuroimaging markers of Alzheimer's disease: systematic review and meta-analysis. J Neurol Neurosurg Psychiatry. 2015;86:127–34.